Thoracic Cancer
Open Access
Thoracic Cancer ISSN 1759-7706

ORIGINAL ARTICLE

Long non-coding RNA XIST expedites lung adenocarcinoma progression through upregulating MDM2 expression via binding to miR-363-3p

Hao Rong[1], Bing Chen[2], Xing Wei[1], Jun Peng[1], Ke Ma[1], Song Duan[3] & Jintao He[1]

1 Department of Thoracic Surgery, Sichuan Cancer Hospital, Chengdu, China
2 Department of Gastroenterology, The First Affiliated Hospital of Zhengzhou University, Zhengzhou, China
3 Department of Pathology, Chongqing Three Gorges Central Hospital, Chongqing, China

Keywords
LAD; MDM2; miR-363-3p; XIST.

Correspondence
J He, Department of Thoracic Surgery, Sichuan Cancer Hospital, No 55, Renmin South Road, Chengdu 610041, China.
Tel: +86131 1189 1080
Email: yddovz@163.com

Received: 31 October 2019;
Accepted: 27 December 2019.

doi: 10.1111/1759-7714.13310

Thoracic Cancer **11** (2020) 659–671

Abstract

Background: Lung adenocarcinoma (LAD) is a highly aggressive malignant tumor which threatens the health and life of the population. Long non-coding RNA X-inactive specific transcript (XIST) and mouse double minute clone 2 (MDM2) are connected with the tumorigenesis of LAD. Nevertheless, whether MDM2 is regulated by XIST has not previously been reported in LAD.

Methods: Quantitative real-time polymerase chain reaction (qRT-PCR) was employed to detect the expression of XIST, microRNA-363-3p (miR-363-3p) and MDM2 in LAD tissues and cells. The proliferation, migration, invasion and apoptosis of LAD cells were determined by 3-(4, 5-dimethylthiazol-2-YI)-2, 5-diphenyltetrazolium bromide (MTT), transwell or flow cytometry assay, respectively. MDM2 protein level was detected using western blot analysis. Dual-luciferase reporter assay, RNA immunoprecipitation (RIP) assay and RNA pulldown assay were performed to determine the interaction among XIST, miR-363-3p and MDM2. A xenograft tumor model was constructed to validate the effect of XIST on LAD cells in vivo.

Results: We found that XIST and MDM2 were remarkably elevated while miR-363-3p was reduced in LAD tissues and cells. Both XIST and MDM2 downregulation restrained proliferation, migration and invasion, and facilitated apoptosis of LAD cells in vitro. Importantly, XIST bound to miR-363-3p to modulate MDM2 expression in LAD cells. Moreover, miR-363-3p knockdown or MDM2 elevation reversed the effects of XIST downregulation on the proliferation, migration, invasion and apoptosis of LAD cells. Furthermore, XIST knockdown constrained tumor growth on LAD cells in vivo.

Conclusions: XIST knockdown repressed proliferation, migration and invasion, and accelerated apoptosis of LAD cells by downregulating MDM2 expression via binding to miR-363-3p.

Key points

Significant findings of the study

1 XIST and MDM2 were abnormally enhanced in LAD tissues and cells.
2 Both downregulation of XIST and MDM2 repressed proliferation, migration and invasion, and boosted apoptosis of LAD cells in vitro.
3 XIST bound to miR-363-3p to regulate MDM2 expression in LAD cells.
4 Downregulation of XIST impeded tumor growth on LAD cells in vivo.

What this study adds

This study confirmed that XIST was a potential target for inhibiting the development of LAD, and affords a possible strategy for the treatment of LAD in the future.

Introduction

Lung cancer is the leading cause of cancer-related deaths worldwide. In 2018, the number of lung cancer deaths was estimated to account for nearly one-fifth (18.4%) of global cancer deaths.[1] According to biological characteristics, lung cancer is mainly classified into small cell lung cancer and non-small cell lung cancer (NSCLC). Lung adenocarcinoma (LAD) is also the most common histological subtype of NSCLC, accounting for approximately 40% of total lung cancer.[2,3] Although treatment has been greatly improved, the five-year overall survival rate of LAD is still less than 15%.[4] Therefore, exploring the molecular mechanisms involved in the occurrence of LAD is critical to the exploitation of novel diagnostic and therapeutic approaches.

Long non-coding RNAs (lncRNAs) are nonprotein encoding RNAs that exert a crucial regulatory role in gene regulatory networks.[5] LncRNA X-inactive specific transcript (XIST) is a major regulator of mammalian X chromosome inactivation.[6] Numerous studies have reported that XIST is connected with the tumorigenesis of a range of tumors, such as colorectal cancer,[7] gastric cancer,[8] pancreatic cancer[9] and hepatocellular cancer.[10] Also, XIST has been shown to facilitate cisplatin resistance in human LAD cells.[11] Nevertheless, the strict molecular mechanism by which XIST influences LAD remains poorly defined.

A class of non-coding RNAs (approximately 18–25 nucleotides)-microRNAs (miRNAs) exert their roles primarily through translational inhibition or mRNA degradation to regulate post-transcriptional gene expression.[12,13] MiRNA-363-3p (miR-363-3p) has been revealed to be abnormally expressed in a series of tumors, such as renal cancer,[14] thyroid cancer,[15] osteosarcoma,[16] and colorectal cancer.[17] Also, miR-363-3p has been shown to be reduced in NSCLC and the decrease of miR-363-3p was connected with gemcitabine resistance.[18,19] To date, the mechanism by which miR-363-3p interacts with XIST is rarely reported in LAD.

Mouse double minute clone 2 (MDM2) is one of the major regulators of the tumor suppressor p53. It has been reported that MDM2 function as an E3 ligase, which expedites malignant tumors by targeting diverse substrates (such as p53) for proteasome-dependent degradation and ubiquitination.[20,21] MDM2 has been revealed to be connected with the occurrence of diverse malignant tumors, such as hepatocellular cancer,[22] papillary thyroid cancer[23] and ovarian cancer.[24] Moreover, MDM2 has been shown to be connected with the tumorigenesis of LAD.[25] Nevertheless, it is not known whether MDM2 is regulated by XIST in LAD.

Consequently, in this study, the expression patterns of XIST and MDM2 in LAD tissue and cells were explored. Moreover, the roles of XIST and MDM2 in LAD cells in vitro were investigated. In addition, the regulatory mechanisms of XIST in adenocarcinoma cells were further studied, and a xenograft tumor model was constructed to confirm the effect of XIST in vivo.

Methods

LAD specimen collection

This research was approved by the Ethics Committee of Sichuan cancer hospital. A total of 35 LAD tissues and surrounding healthy lung tissues were converged from Sichuan cancer hospital for LAD study. All patients with LAD who participated in the study received written informed consents and they did not receive radiotherapy or chemotherapy before surgery.

Cell culture

LAD cells A549 and H1299, as well as human normal lung epithelial cells BEAS-2B, were procured from American Tissue Culture Collection (Manassas, VA, USA). The Roswell Park Memorial Institute (RPMI) 1640 medium (A1049101, Gibco, Grand Island, NY, USA) was utilized to culture the above cell lines. Furthermore, fetal bovine serum (10%, FBS, 10099-141, Gibco) and streptomycin/penicillin (1%, HyClone, Logan, UT, USA) were added to the RPMI 1640 medium (Gibco) to culture the cells. All cells were kept in an incubator with 5% CO_2 at 37°C.

Quantitative real-time polymerase chain reaction (qRT-PCR)

The TRIzol Reagent (15596018) from Thermo Fisher Scientific (Waltham, MA, USA) was utilized for the acquirement of total RNA of LAD tissues and surrounding healthy lung tissues as well as LAD cells. The MiRNA Reverse Transcription kit (4 366 597, Thermo Fisher

Scientific) or High-Capacity complementary DNA Reverse Transcription kit (4 374 967, Thermo Fisher Scientific) was employed for the synthesis of the first-strand complementary DNA of miR-363-3p, XIST and MDM2, respectively. The SYBR Premix Dimer Eraser Kit (RR091A) from Takara (Dalian, China) was employed to carry out qRT-PCR. The primers were exhibited as follows: glyceraldehyde-3-phosphate dehydrogenase (GAPDH) (F: 5′-GAAGGTGAA GGTCGGAGTC-3′, R: 5′-GAAGATGGTGATGGGATTTC-3′), U6 small nuclear RNA (snRNA) (F: 5′-GCTCGCTTCG GCAGCACA-3′, R: 5′-GAGGTATTCGCACCAGAGGA-3′),

XIST (F: 5′-CAGACGTGTGCTCTTC-3′, R: 5′-CGAT CTGTAAGTCCACCA-3′), miR-363-3p (F: 5′-GCCGAGAA TTGCACGGTAT-3′, R: 5′-CTCAACTGGTGTCGTGGA-3′) as well as MDM2 (F: 5′-GAATCATCGGACTCAGG TACATC-3′, R: 5′-TCTGTCTCACTAATTGCTCTCCT-3′). The levels of XIST, MDM2 and miR-363-3p were computed through $2^{-\Delta\Delta Ct}$ method, and GAPDH or U6 snRNA served as an internal control.

Cell transfection

Short hairpin RNA targeting XIST (sh-XIST), short hairpin RNA targeting MDM2 (sh-MDM2) and negative control (sh-control, Sigma-SHC002V) were procured from Sigma Aldrich (St. Louis, Missouri, USA). The pcDNA3.1/XIST overexpression vector (pcDNA3.1/XIST) and pcDNA3.1/MDM2 overexpression vector (pcDNA3.1/MDM2) were constructed using the pcDNA3.1 vector (K480001) (Invitrogen, Carlsbad, CA, USA). MiRNA mimics targeting miR-363-3p (miR-363-3p mimics) and scrambled mimics control (NC-mimics) as well as miRNA inhibitor targeting miR-363-3p (miR-363-3p inhibitor) and scrambled mimics control (NC-inhibitor) were obtained from Ambion lnc (Austin, TX, USA). Lipofectamine 2000 reagent (Invitrogen) was applied to transfect oligonucleotides or plasmids into LAD cells transiently. The sequences were displayed as the following: sh-XIST (5′-CCGGGCU GACUACCAGAGAUUUACTCGAGTAAATCTCAGGT-AGTCAGCTTTTTG-3′), sh-MDM2 (5′-UUGGUAUUG CACAUUUGCCUG-3′), NC-mimics (5′-AUUGGAACGA UACAGAGAAGAUU-3′), miR-363-3p mimics (5′-AAUU GCACGGUAUCCAUCUGUAUU-3′), NC-inhibitor (5′-U UCUCCGAACGUGUCACGUTT-3′) as well as miR-363-3p inhibitor (5′-UACAGAUGGAUACCGUGCA AUU-3′).

3-(4, 5-dimethylthiazol-2-YI)-2, 5-diphenyltetrazolium bromide (MTT) assay

The proliferation of transfected LAD cells was assessed with MTT assay. Briefly, the 96-well plates (3917) (Corning Costar, Corning, NY, USA) were employed to seed transfected LAD cells with 3×10^3 cells in each well for 24 hours, 48 hours and 72 hours. Subsequently, each well was replenished with MTT (11 465 007 001, 20 μL, Sigma Aldrich) and maintained for four hours. After discarding the supernatant, dimethyl sulfoxide (472 301, 150 μL, Sigma Aldrich) was replenished to each well for the dissolution of the formazan crystals. A Microplate Absorbance Reader (Thermo Fisher Scientific) was used to evaluate the color reaction at 490 nm.

Transwell assay

The transwell chamber (8 μm, Corning Costar) was utilized for the assessment of the migratory and invasive capacities of transfected LAD cells. The invasion assay of transfected LAD cells was similar to the migration assay but using a transwell chamber coated with matrigel matrix (BD Biosciences, San Jose, CA, USA). Briefly, RPMI 1640 medium containing transfected LAD cells (4×10^4/100 μL) was added to the upper chamber, while FBS (10%) supplemented with RPMI 1640 medium was added as a chemoattractant to the lower chamber. After culturing for 48 hours in an incubator with 5% CO_2 at 37°C, the cells on the upper surface of the member were removed with a cotton swab. Following this, the migrated or invaded cells of the lower surface of the membrane were fixed via methanol (100%) and stained with 0.1% crystal violet. Finally, a light microscope from Olympus (Tokyo, Japan) was employed for counting the migrated or invaded cells.

Flow cytometry assay

The Annexin V-fluorescein isothiocyanate (FITC)/propidium iodide (PI) apoptosis detection kit (APOAF-20TST, Sigma Aldrich) was employed to assess the apoptosis rate of transfected LAD cells. Briefly, transfected LAD cells (1×10^6) cultured for 48 hours were washed and resuspended in binding buffer. Annexin V-FITC (10 μL) and PI (5 μL) were then supplemented and incubated for 15 minutes in the dark. Finally, the FACScan flow cytometry (BD Biosciences) was utilized for analysis of the apoptosis rate of transfected LAD cells.

Dual-luciferase reporter assay

The starbase database was employed to predict the binding sites between XIST or MDM2 and miR-363-3p. After that, the wild-type XIST and mutant XIST sequences harboring predicted miR-363-3p binding sites were synthesized and inserted into the pGL3-control vector (E1741, Promega, Madison, WI, USA) to construct the luciferase reporter vector of XIST-WT and XIST-Mut. Similarly, the wild-type

MDM2 3'-untranslated regions (UTR) and mutant MDM2 3'-UTR sequences containing embracing predicted miR-363-3p binding sites were synthesized and inserted into the pGL3-control vector for the construction of the luciferase reporter vectors of MDM2-WT and MDM2-Mut. Following this, the luciferase reporter vectors were cotransfected into LAD cells with NC-mimics or miR-363-3p mimics for the execution of the dual-luciferase reporter assay, respectively. Finally, the luciferase activities of luciferase reporter vectors were evaluated via the dual-luciferase reporter assay kit (Promega).

RNA immunoprecipitation (RIP) assay

The interaction between XIST or MDM2 and miR-363-3p was analyzed with Magna RIP kit (MAGNARIP01, Millipore, Bedford, MA, USA). Originally, LAD cells were lysed in RIP lysis buffer with protease-inhibitor cocktail (1 842 196, Hoffman-La Roche, Basel, Switzerland) and RNase inhibitor (EO0381, Thermo Fisher Scientific). Subsequently, the lysates of LAD cells were incubated in a RIP buffer harboring protein A/G magnetic beads conjugated IgG (PP64B, Millipore) or Ago2 antibody (03–110, Millipore). Finally, the enrichments of XIST, miR-363-3p and MDM2 in precipitates were measured with qRT-PCR.

RNA pulldown assay

The biotinylated (Bio)-NC, Bio-miR-363-3p-Mut and Bio-miR-363-3p-WT were obtained from Sigma Aldrich. The lysates of LAD cells were then mixed with biotinylated (Bio)-NC, Bio-miR-363-3p-WT or Bio-miR-363-3p-Mut, respectively. Following this, streptavidin-coupled magnetic beads were added to the above mixtures for two hours. Finally, the level of XIST was assessed through qRT-PCR.

Western blot analysis

First, the whole proteins of LAD tissues and surrounding healthy lung tissues as well as LAD cells were extracted with radio-immunoprecipitation assay (RIPA) lysis buffer (2114–500, Thermo Fisher Scientific). Next, the sodium dodecyl sulphate-polyacrylamide gel electrophoresis (89 888, 10%, SDS-PAGE, Thermo Fisher Scientific) was utilized for the separation of the total protein. Following this, isolated proteins were transferred onto polyvinylidene difluoride (PVDF) membranes (Millipore). The PVDF membranes were then obstructed through tris-buffered saline Tween (TBST) buffer with 5% skim milk. The PVDF membranes were incubated with primary antibodies: anti-MDM2 (1:1000, ab38618, Abcam, Cambridge, MA, USA) and anti-GAPDH (1:2500, ab9485, Abcam). After washing, the membranes were incubated with goat anti-rabbit IgG (1:2000, ab205718, Abcam). GAPDH was regarded as a loading control. Finally, the ImageJ software from the National Institutes of Health (Bethesda, MD, USA) was used for visualizing the bands.

In vivo experiment

The animal experiments were approved by the Ethics Committee of Sichuan cancer hospital. A total of 10 BALB/c nude mice (five-week-old) from Shanghai Experimental Animal Center (Shanghai, China) were assigned to two groups: the sh-control group (injected with A549 cells transfected with sh-control) and the sh-XIST group (injected with A549 cells transfected with lentivirus-mediated sh-XIST). Briefly, the dorsal side of each nude mouse was subcutaneously injected with A549 cells (1×10^7) transfected with sh-control or lentivirus-mediated sh-XIST. A digital caliper was used to measure the tumor volume once per week. The tumor volume was calculated with the equation: Volume = (length $\times$width^2)/2. After four weeks, the mice were euthanized under anesthesia to separate the tumor tissues for tumor weighing.

Statistical analysis

SPSS 18.0 software (SPSS, Chicago, IL, USA) and GraphPad Prism 6.0 (GraphPad, San Diego, CA, USA) were utilized for the execution of the statistical analysis. Differences with $P < 0.05$ were statistically significant. Student's *t*-test or one-way variance analysis (ANOVA) was employed for comparing the differences between two or among more groups. Data exhibited as mean $\pm$ standard deviation were derived from three independent experiments.

Results

Downregulation of XIST impeded proliferation, migration and invasion, and expedited apoptosis of LAD cells in vitro

To determine the role of XIST in LAD, we first examined the expression level of XIST in 35 LAD tissues and surrounding healthy lung tissues via qRT-PCR. The results exhibited that a conspicuous elevation of XIST was observed in LAD tissues compared to surrounding healthy lung tissues (Fig 1a). Subsequently, the level of XIST in LAD cells was measured with qRT-PCR. As displayed in Fig 1b, XIST was remarkably increased in both A549 and H1299 cells in comparison with the BEAS-2B cells. Following this, sh-XIST, sh-control, pcDNA3.1 or pcDNA3.1/XIST was transfected into A549 and H1299 cells to silence or augment the expression of XIST, respectively. Results of

qRT-PCR confirmed that the expression of XIST was markedly reduced in A549 and H1299 cells transfected with sh-XIST compared with the control group, while the expression of XIST was distinctly enhanced in A549 and H1299 cells transfected with pcDNA3.1/XIST (Fig 1c). The effects of XIST on proliferation, migration, invasion and apoptosis of LAD cells were then further studied. MTT assay was performed and the results exhibited that the reduction of XIST strikingly impeded cell proliferation in both A549 and H1299 cells (Fig 1d,e). Transwell assay displayed that the number of migration and invasion of A549 and H1299 cells induced by XIST silencing was obviously reduced (Fig 1f,g). Moreover, flow cytometry assay revealed that an apparent augmentation in apoptosis rate was discovered in A549 and H1299 cells following downregulation of XIST expression (Fig 1h). Taken together, these results indicated that XIST knockdown restrained cell proliferation, migration and invasion, and expedited cell apoptosis in LAD cells in vitro.

XIST directly interacted with miR-363-3p in LAD cells

To investigate the regulatory mechanism of XIST on cell proliferation, migration, invasion and apoptosis in LAD cells, the starbase database was employed to predict the underlying molecular mechanism. As presented in Fig 2a, miR-363-3p possessed complementary base pairs with XIST. Moreover, we found that miR-363-3p was prominently decreased in LAD tissues compared to that in surrounding healthy lung tissues (Fig 2b). Consistently, a significant reduction of miR-363-3p was observed in A549 and H1299 cells versus BEAS-2B cells (Fig 2c). In addition,

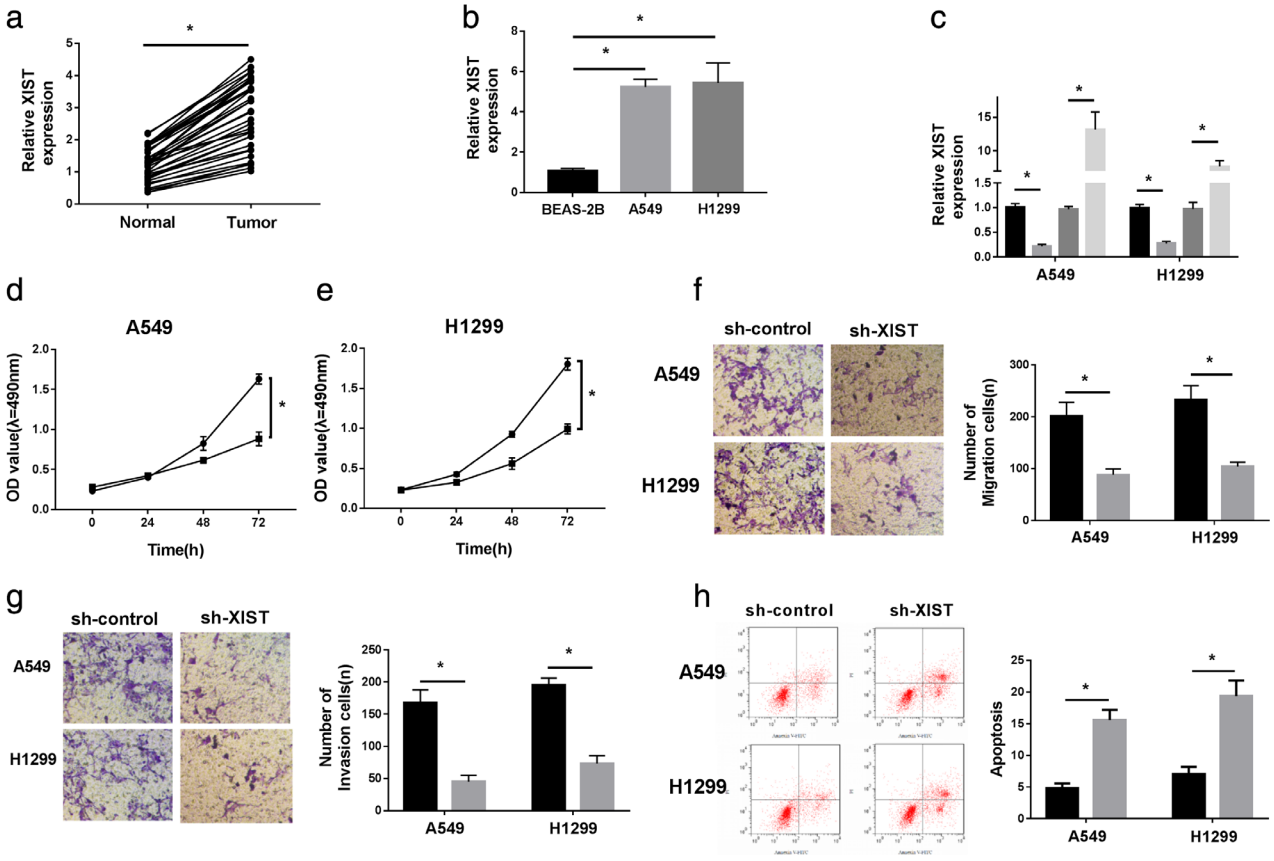

Figure 1 Effects of downregulation of XIST on proliferation, migration, invasion and apoptosis of LAD cells. (**a**) The expression levels of XIST in 35 LAD tissues and surrounding healthy lung tissues were detected using qRT-PCR. (**b**) QRT-PCR was employed to analyze the expression level of XIST in A549, H1299 and BEAS-2B cells. (**c**) After sh-XIST, sh-control, pcDNA3.1 or pcDNA3.1/XIST transfection, the expression level of XIST in A549 and H1299 cells was assessed by qRT-PCR. (■) sh-control, (■) sh-XIST, (■) pcDNA3.1, (■) pcDNA3.1/XIST. (**d** and **e**) After sh-XIST or sh-control transfection, the proliferation of A549 and H1299 cells was determined with MTT assay. (—●—) sh-control, (—■—) sh-XIST. (**f** and **g**) The migration and invasion activities of A549 and H1299 cells transfected with sh-XIST or sh-control were evaluated with a transwell assay. (■) sh-control, (■) sh-XIST. (**h**) The apoptosis rates of A549 and H1299 cells transfected with sh-XIST or sh-control were assessed by flow cytometry assay. $*P < 0.05$. (■) sh-control, (■) sh-XIST.

the downregulation of XIST obviously enhanced the expression of miR-363-3p in A549 and H1299 cells in comparison with the control group (Fig 2d). Subsequently, the luciferase reporter vectors were constructed and cotransfected with miR-363-3p-mimics or NC-mimics into A549 and H1299 cells to verify whether XIST was a sponge of miR-363-3p. Results of the dual-luciferase reporter assay exhibited that the luciferase activity of XIST-WT in A549 and H1299 cells was drastically reduced by miR-363-3p-mimics compared to the control group, whereas XIST-Mut constrained this effect (Fig 2e,f). In addition, RIP assay and RNA pulldown assay were employed to further confirm the interaction between XIST and miR-363-3p in A549 and H1299 cells. RIP assay confirmed that XIST and miR-363-3p were remarkably enriched in Ago2-containing beads in comparison to those harboring control immunoglobulin G antibody (Fig 2g,h). Furthermore, RNA pulldown assay revealed that XIST was strikingly enriched in Bio-miR-363-3p-WT compared to that in Bio-miR-363-3p-Mut group with broken XIST binding sites (Fig 2i). In summary, these data indicated that XIST directly interacted with miR-363-3p in A549 and H1299 cells.

Silencing of MDM2 blocked proliferation, migration and invasion, and boosted apoptosis of LAD cells in vitro

To explore the involvement of MDM2 in LAD, we evaluated the expression of MDM2 mRNA and protein in 35 LAD tissues and surrounding healthy lung tissues through qRT-PCR and western blot analysis. In comparison with normal lung tissues, the levels of MDM2 mRNA

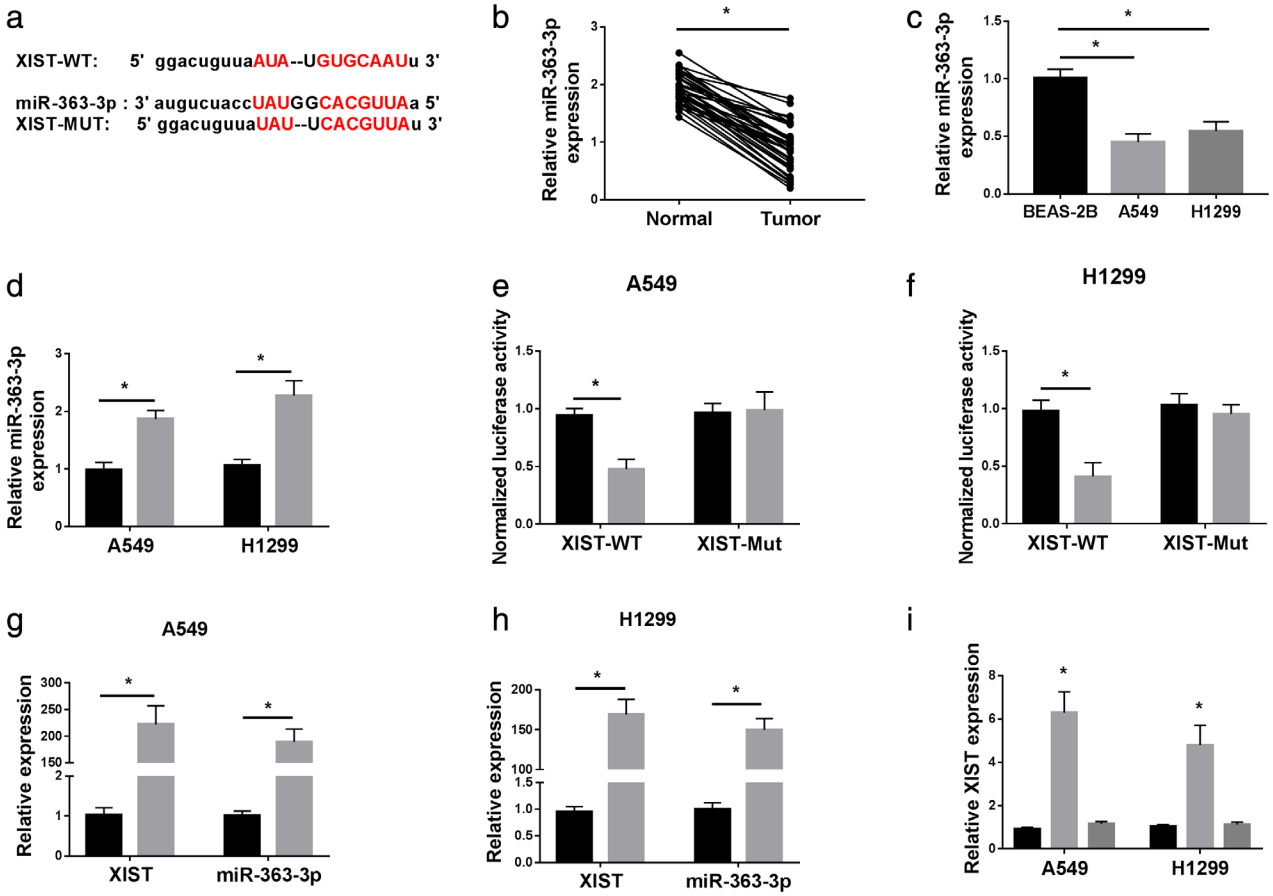

Figure 2 Interaction between XIST and miR-363-3p in LAD cells. (**a**) XIST and miR-363-3p binding sites were predicted with the starbase database. (**b**) QRT-PCR was employed to analyze the expression level of XIST in 35 LAD tissues and surrounding healthy lung tissues. (**c**) The levels of miR-363-3p in A549, H1299 and BEAS-2B cells were evaluated by qRT-PCR. (**d**) After sh-XIST or sh-control transfection, the levels of miR-363-3p in A549 and H1299 cells were determined with qRT-PCR. (■) sh-control, (■) sh-XIST. (**e** and **f**) Dual-luciferase reporter assay was employed to assess the luciferase activity of luciferase reporter vectors in A549 and H1299 cells transfected with miR-363-3p mimics or NC-mimics. (■) NC-mimics, (■) miR-363-3p-mimics. (**g** and **h**) Targeting the relationship between XIST and miR-363-3p was detected by RIP assay. (■) Anti-gG, (■) Anti-Ago2. (**i**) RNA pulldown assay was employed for the assessment of the interaction between XIST and miR-363-3p. The biotinylated XIST, miR-363-3p or control was transfected into A549 and H1299 cells. *$P < 0.05$. (■) Bio-NC, (■) Bio-miR-363-3p-WT, (■) Bio-miR-363-3p-Mut.

and protein were evidently enhanced in LAD tissues (Fig 3a,b). Next, the levels of MDM2 mRNA and protein in LAD cells and BEAS-2B cells were detected by qRT-PCR and western blot analysis. The results indicated that MDM2 mRNA and protein were apparently upregulated in A549 and H1299 cells in comparison to that in BEAS-2B cells (Fig 3c,d). Besides, sh-MDM2 or sh-control was transfected into A549 and H1299 cells to impede the expression of MDM2. Western blot analysis was then employed and the results displayed that the protein level of MDM2 was remarkably decreased in A549 and H1299 cells compared to the control group (Fig 3e). Following this, the effects of MDM2 knockdown on the proliferation, migration, invasion and apoptosis of A549 and H1299 cells was studied. MTT assay was then utilized to evaluate cell proliferation and the results showed that MDM2 reduction strikingly repressed the proliferation of A549 and H1299 cells than the control group (Fig 3f,g). Similar results were observed in the transwell assay where decreased MDM2 expression blocked the migration and invasion abilities of A549 and H1299 cells (Fig 3h,i). Furthermore, flow cytometry assay was applied and the data exhibited that the downregulation of MDM2 accelerated cell apoptosis in A549 and H1299 cells (Fig 3j). Overall, these results revealed that MDM2 downregulation blocked cell proliferation, migration and invasion, and facilitated cell apoptosis in LAD cells in vitro.

XIST regulated MDM2 expression by binding to miR-363-3p in LAD cells

Considering that lncRNA functions as a competing endogenous RNA (ceRNA), we hypothesized that XIST could regulate the expression of MDM2 in LAD cells by sponging miR-363-3p. To verity this hypothesis, we predicted the binding sites between MDM2 and miR-363-3p using the starbase database. As displayed in Fig 4a, MDM2 held potential binding sits for miR-363-3p. We then established wild-type 3'-UTR of MDM2 luciferase reporter vector (MDM2-WT) harboring the target sites of miR-363-3p and mutant 3'-UTR of MDM2 luciferase reporter vector (MDM2-Mut). Dual-luciferase reporter assay exhibited that the luciferase activity of MDM2-WT was evidently decreased by miR-363-3p mimics compared with the control group, while pcDNA3.1/XIST abolished the inhibitory effect of miR-363-3p mimics on MDM2-WT activity (Fig 4b,c). Furthermore, RIP assay was applied and the results showed that XIST, miR-363-3p and MDM2 were enriched in miRNA ribonucleoprotein complexes in comparison with the control immunoglobulin G antibody (Fig 4d,e). In addition, sh-control, sh-XIST, sh-XIST+NC inhibitor or sh-XIST+miR-363-3p inhibitor was transfected into A549 and H1299 cells to explore the effects of XIST and miR-363-3p on MDM2 expression. The results of qRT-PCR showed that reduced XIST expression remarkably inhibited the expression of MDM2 in both A549 and H1299 cells, whereas reduction of miR-363-3p partially reversed this effect (Fig 4f). Western blot analysis confirmed that the expression level of MDM2 protein was prominently reduced by XIST knockdown, while this decrease was partly overturned by the inhibition of miR-363-3p (Fig 4g,h). In conclusion, we revealed that XIST could regulate MDM2 expression by binding to miR-363-3p in LAD cells.

MiR-363-3p inhibition or MDM2 overexpression reversed the effects of XIST knockdown on the proliferation, migration, invasion and apoptosis of LAD cells

In consideration of the above results, we further understood the relationship between XIST and miR-363-3p or MDM2 in biological functions of LAD via executing rescue experiments by reducing miR-363-3p or augmenting MDM2 in LAD cells with XIST knockdown. MTT assay was performed and the results confirmed that the inhibitory effect of XIST knockdown on the proliferation of A549 and H1299 cells was reversed by miR-363-3p reduction or MDM2 overexpression (Fig 5a,b). Also, transwell assay revealed that miR-363-3p downregulation or MDM2 augmentation overturned the inhibitory effect of XIST silencing on migration and invasion of A549 and H1299 cells (Fig 5c,d). In addition, flow cytometry assay indicated that the acceleration of apoptosis by XIST inhibition was recovered by reduced miR-363-3p or enhanced MDM2 (Fig 5e,f). Together, these results revealed that XIST downregulation affected LAD biological functions by binding to miR-363-3p and mediating MDM2 expression.

Knockdown of XIST impeded tumor growth of LAD cells in vivo

To confirm the role of XIST on tumor in vivo, we injected A549 cells transfected with sh-control or lentivirus-mediated sh-XIST into nude mice to construct xenograft tumor models. Four weeks after inoculation, the tumor tissues of the nude mice were surgically cut to determine the weight and volume of the tumor. The data and images indicated that the weight and volume of tumor were markedly reduced in the sh-XIST group compared with that in the control group (Fig 6a,b). Moreover, the levels of XIST and miR-363-3p in tumor were detected by qRT-PCR. Compared to the control group, XIST was strikingly decreased and miR-363-3p was remarkably enhanced in the lentivirus-mediated sh-XIST group (Fig 6c,d).

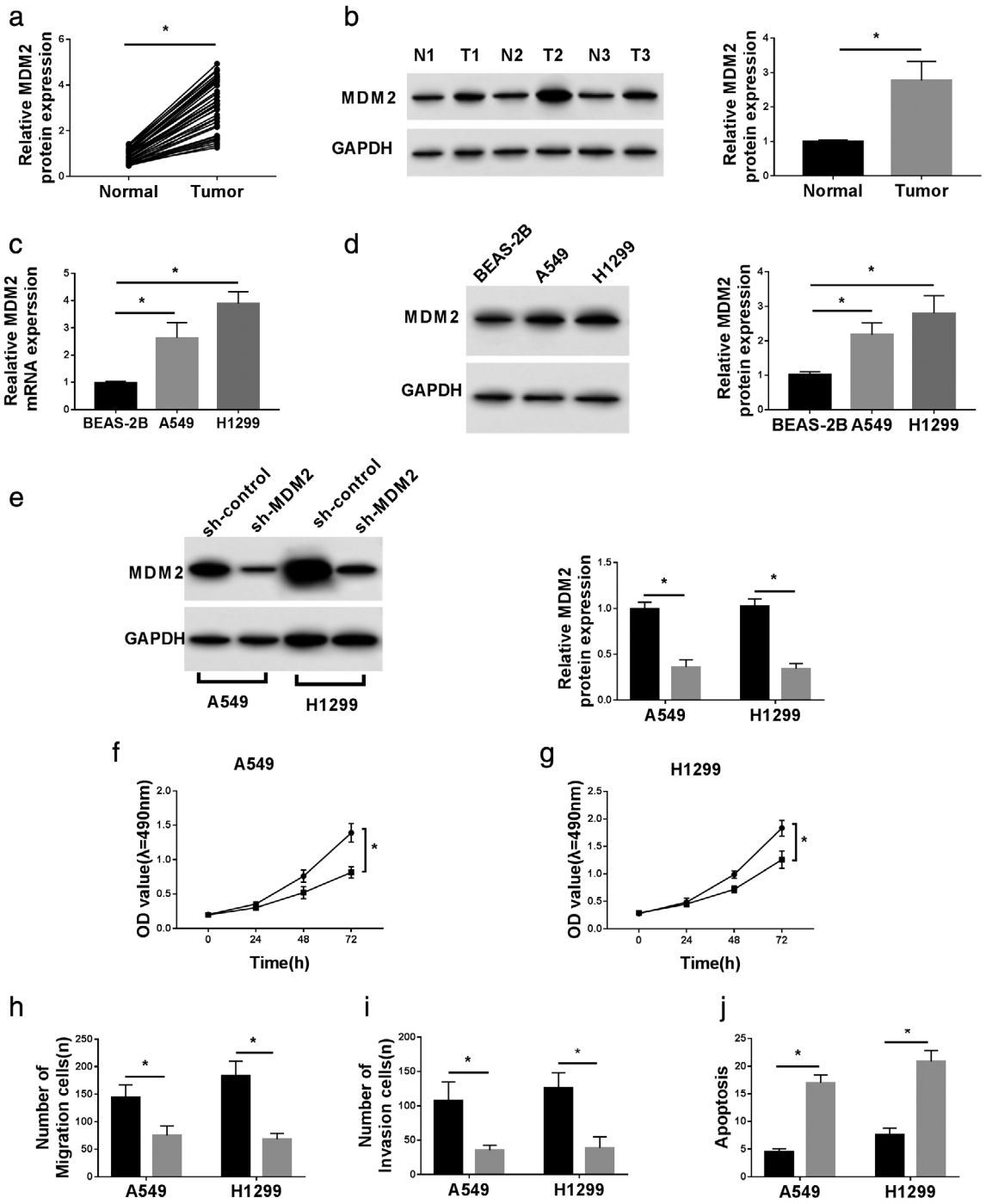

Figure 3 MDM2 downregulation repressed proliferation, migration and invasion, and boosted apoptosis of LAD cells. (**a** and **b**) The levels of MDM2 mRNA and protein in 35 LAD tissues and surrounding healthy lung tissues were assessed with qRT-PCR or western blot analysis. (**c** and **d**) QRT-PCR or western blot analysis was employed for detection of the expression levels of MDM2 mRNA and protein in A549, H1299 and BEAS-2B cells. (**e**) Western blot analysis of MDM2 protein expression in A549 and H1299 cells transfected with sh-control or sh-MDM2. (■) sh-control, (■) sh-MDM2. (**f** and **g**) MTT assay was employed for the determination of the proliferation of A549 and H1299 cells transfected with sh-control or sh-MDM2. (—●—) sh-control, (—■—) sh-MDM2. (**h** and **i**) The migration and invasion of A549 and H1299 cells transfected with sh-control or sh-MDM2 were evaluated by transwell assay. (■) sh-control, (■) sh-MDM2. (**j**) Flow cytometry assay was performed to assess the apoptosis of A549 and H1299 cells transfected with sh-control or sh-MDM2. $*P < 0.05$. (■) sh-control, (■) sh-MDM2.

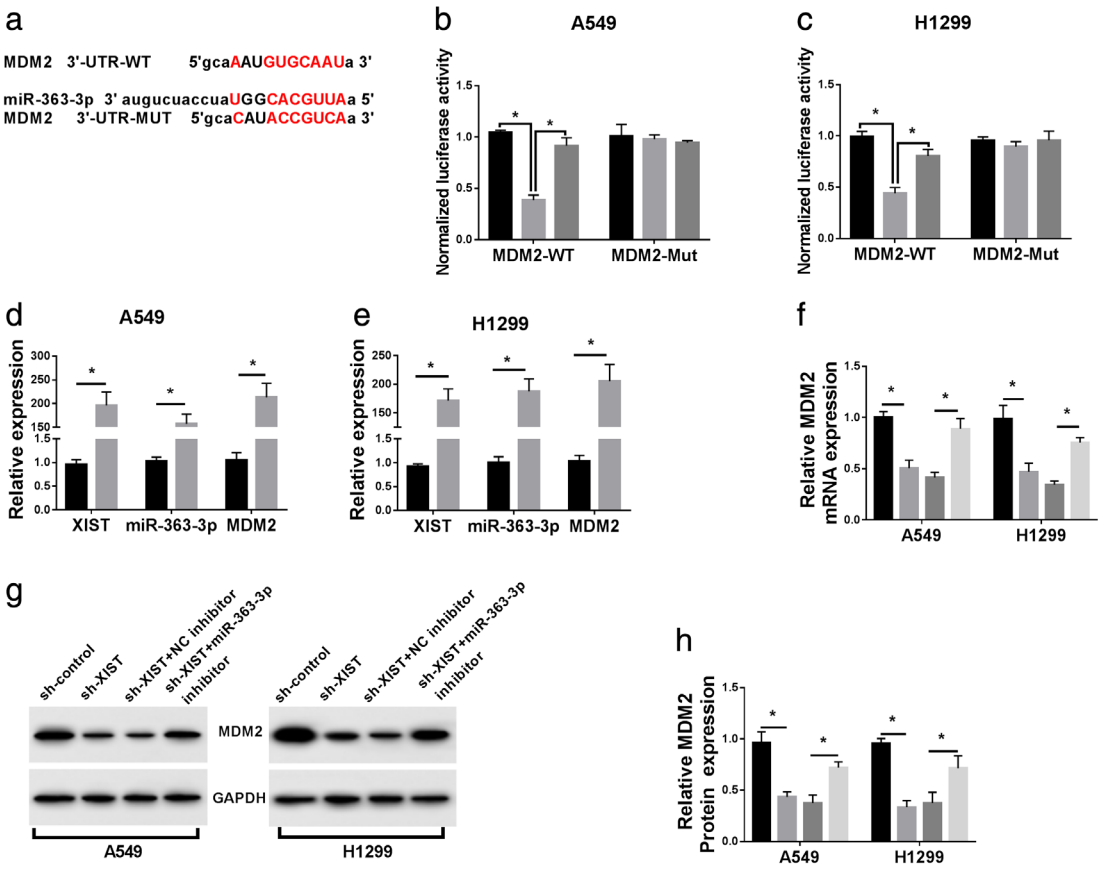

Figure 4 XIST targeted miR-363-3p to regulate MDM2 expression in LAD cells. (**a**) The binding sites of miR-363-3p in MDM2 were predicted by employing the starbase database. (**b** and **c**) The luciferase activities of MDM2-WT or MDM2-Mut in A549 and H1299 cells transfected with NC-mimics+pcDNA3.1, miR-363-3p mimics+pcDNA3.1 or miR-363-3p mimics+pcDNA3.1/XIST were measured with a dual-luciferase reporter assay. (■) NC-mimics+pcDNA3.1, (■) miR-363-3p mimics+pcDNA3.1, (■) miR-363-3p mimics+pcDNA3.1/XIST. (**d** and **e**) RIP assay was performed in A549 and H1299 cells and the coprecipitated RNA was analyzed with qRT-PCR. (■) Anti-IgG, (■) Anti-Ago2. (**f**) The level of MDM2 mRNA in A549 and H1299 cells transfected with sh-control, sh-XIST, sh-XIST+NC inhibitor or sh-XIST+miR-363-3p inhibitor was detected using qRT-PCR. (■) sh-control, (■) sh-XIST, (■) sh-XIST+NC inhibitor, (■) sh-XIST+miR-363-3p inhibitor. (**g** and **h**) Western blot analysis of MDM2 protein level in A549 and H1299 cells transfected with sh-control, sh-XIST, sh-XIST+NC inhibitor or sh-XIST+miR-363-3p inhibitor. *$P < 0.05$. (■) sh-control, (■) sh-XIST, (■) sh-XIST+NC inhibitor, (■) sh-XIST+miR-363-3p inhibitor.

Furthermore, the levels of MDM2 mRNA and protein were assessed by qRT-PCR or western blot analysis. We observed that MDM2 mRNA and protein were markedly decreased in the sh-XIST group compared with that in the control group (Fig 6e–g). Collectively, these results indicated that XIST silencing impeded tumor growth of LAD cells in vivo, which was consistent with the in vitro results.

Discussion

LAD is a malignant tumor with a high degree of invasiveness and rapid lethality.[26] LncRNAs exert crucial roles in gene regulation, which affects cell homeostasis by affecting cell survival, migration, proliferation, or genomic stability.[27] It has been reported that lncRNAs can be used as a minimally invasive diagnostic/prognostic biomarker and therapeutic target in a range of cancers.[28] As a result, the role of XIST in LAD and its molecular regulatory mechanisms were explored.

Recent studies have stated that XIST acts as an oncogene in a variety of cancers. For example, Wei *et al.* revealed that XIST was abnormally elevated in pancreatic cancer tissues and cells, and increased XIST expression expedited cell proliferation in pancreatic cancer cells.[9] Furthermore, a remarkable enhancement of XIST was observed in colorectal cancer tissues and cells, and reduced XIST expression impeded the proliferation, epithelial-mesenchymal transition (EMT) and invasion of colorectal cancer cells in vitro, and repressed tumor metastasis and growth in vivo. In the current research, an apparent increase of XIST was

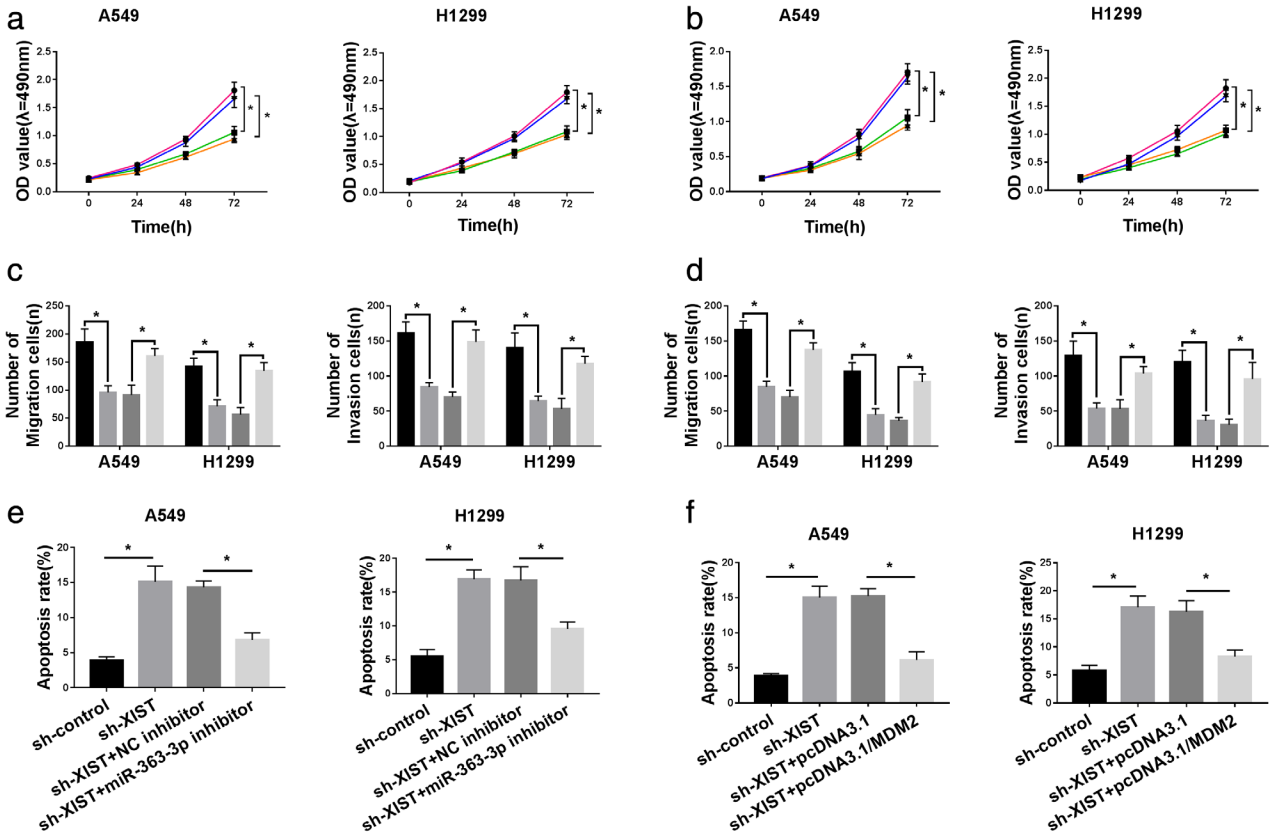

Figure 5 XIST affected LAD cells via binding to miR-363-3p to mediate MDM2 expression. (**a** and **b**) MTT assay revealed that miR-363-3p knockdown or MDM2 augmentation rescued the inhibitory effect of XIST inhibition in A549 and H1299 cells. (**c** and **d**) Transwell assay demonstrated that miR-363-3p reduction or MDM2 enhancement reversed the suppressive impact of XIST downregulation on cell migration and invasion in A549 and H1299 cells. (**e** and **f**) Flow cytometry assay implied that miR-363-3p downregulation or MDM2 elevation overturned the accelerative influence of XIST reduction on the apoptosis of A549 and H1299 cells. $^*P < 0.05$. (a) (—●—) sh-control, (—■—) sh-XIST, (—▲—) sh-XIST+NC inhibitor, (—▼—) sh-XIST+miR-363-3p inhibitor. (b) (—●—) sh-control, (—■—) sh-XIST, (—▲—) sh-XIST+pcDNA3.1, (—▼—) sh-XIST+pcDNA3.1/MDM2. (c) (■) sh-control, (■) sh-XIST, (■) sh-XIST+NC inhibitor, (■) sh-XIST+miR-363-3p inhibitor. (d) (■) sh-control, (■) sh-XIST, (■) sh-XIST+pcDNA3.1, (■) sh-XIST+pcDNA3.1/MDM2.

discovered in LAD tissues and cells. Moreover, XIST reduction restrained the proliferation, migration and invasion, and triggered apoptosis in LAD cells in vitro and blocked tumor growth in vivo. One report from Sun *et al.* revealed that XIST was robustly augmented in LAD cells with cisplatin resistance, and increased XIST expression enhanced the chemo-resistance of LAD cells to cisplatin in vitro and in vivo by blocking apoptosis and expediting proliferation.[11] Our results revealed that XIST exerted a carcinogenic role in LAD, and this conclusion is consistent with the above study.

Tay *et al.* showed that lncRNA might act as a molecular sponge of miRNA to exert its biological functions, thereby regulating the expression of miRNA target genes.[29] In the present study, the starbase database was employed for the prediction of the binding sites between XIST and miR-363-3p. A report by Jiang *et al.* stated that miR-363-3p was prominently decreased in NSCLC cells and tissues, and the enhancement of miR-363-3p constrained the invasion and proliferation of NSCLC cells.[30] Furthermore, Chang *et al.* stated that the augmentation of miR-363-3p refrained cell invasion, migration and EMT in NSCLC cells.[19] In the present study, we further confirmed that XIST directly bound to miR-363-3p by dual-luciferase reporter assay, RIP assay and RNA pulldown assay. Moreover, miR-363-3p was drastically decreased in LAD tissues and cells, and reduced miR-363-3p expression recovered the effects of XIST downregulation on cell proliferation, migration, invasion and apoptosis in LAD cells. Our results are consistent with the above studies, revealing that miR-363-3p exerted an anticancer role in LAD.

It is known that miRNA negatively regulates gene expression basically via binding to the 3'-UTR of a target gene.[31] In the current study, MDM2 possessed potential

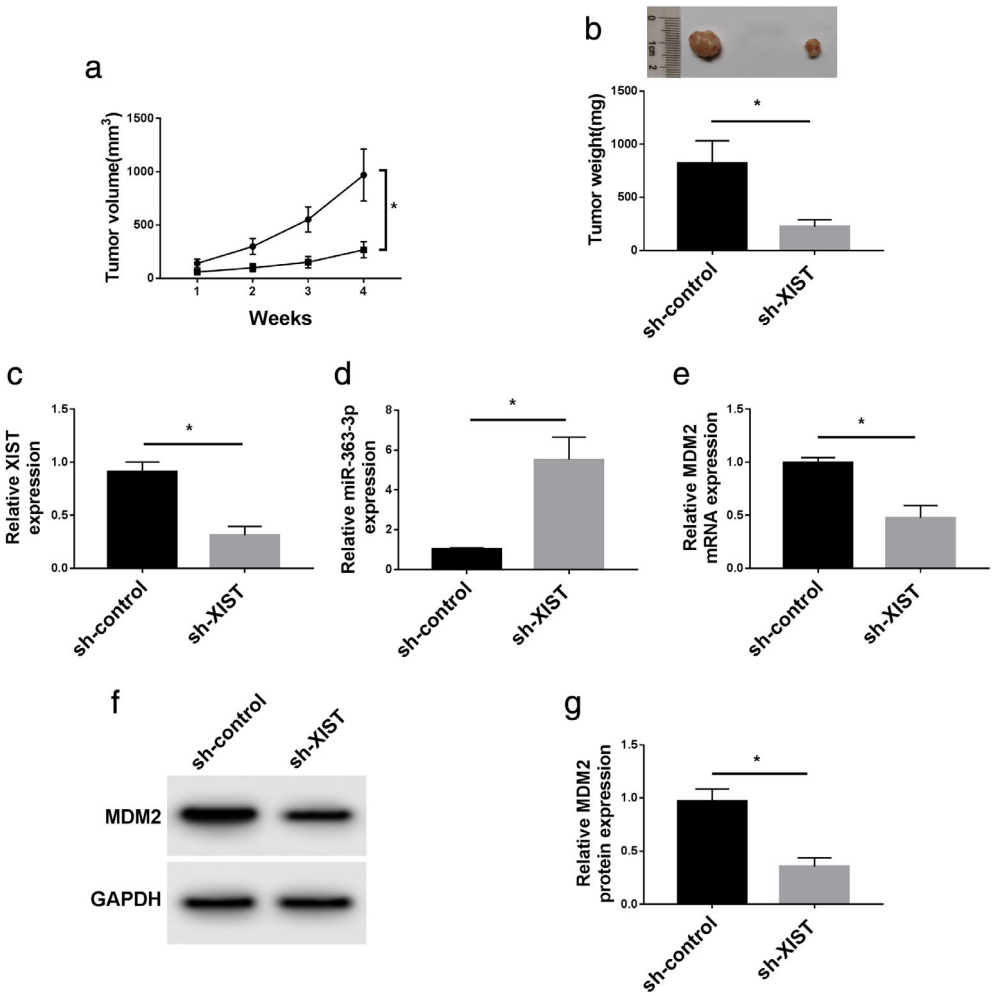

Figure 6 Downregulation of XIST retarded tumor growth of LAD cells in vivo. (**a** and **b**) The volume and weight of the lentivirus-mediated sh-XIST group were remarkably diminished compared with those of the sh-control group. (–●–) sh-control, (–■–) sh-XIST. (**c** and **d**) The level of XIST was evidently decreased while miR-363-3p was obviously enhanced in the sh-XIST group compared with the sh-control group. (**e**–**g**) The levels of MDM2 mRNA and protein were drastically reduced in the lentivirus-mediated sh-XIST group compared with those in the sh-control group. $*P < 0.05$.

binding sites for miR-363-3p was discovered using the starbase database. The study by Tang *et al.* revealed that a noticeable acceleration of MDM2 was observed in LAD tissues and cells, and augmented MDM2 expression boosted the invasion, migration and proliferation of LAD cells.[25] The report by Zhang *et al.* showed that MDM2 was prominently upregulated in stage III and stage IV of rat lung cancer and elevated MDM2 expression might connect with the metastasis and progression of lung cancer.[32] In the present study, MDM2 was strikingly enhanced in LAD tissues and cells. Importantly, we revealed that XIST directly bound to miR-363-3p to regulate MDM2 expression with dual-luciferase reporter assay, RIP assay as well as western blot analysis. In addition, MDM2 augmentation could overturn the effects of XIST inhibition on cell proliferation, migration, invasion and apoptosis in LAD cells. We revealed that MDM2 was an oncogene of LAD which is consistent with the results of the studies by Tang *et al.* [25] and Zhang *et al.* [32] From all these findings, we concluded that XIST modulated LAD progression by regulating MDM2 expression via miR-363-3p (Fig 7).

In conclusion, XIST and MDM2 were augmented in LAD tissues and cells. Interestingly, knockdown of XIST impeded cell proliferation, migration and invasion, and boosted cell apoptosis through reducing MDM2 expression via binding to miR-363-3p in LAD cells. This study confirmed that XIST was a potential target for inhibiting the development of LAD, and affords a possible strategy for the treatment of LAD in the future.

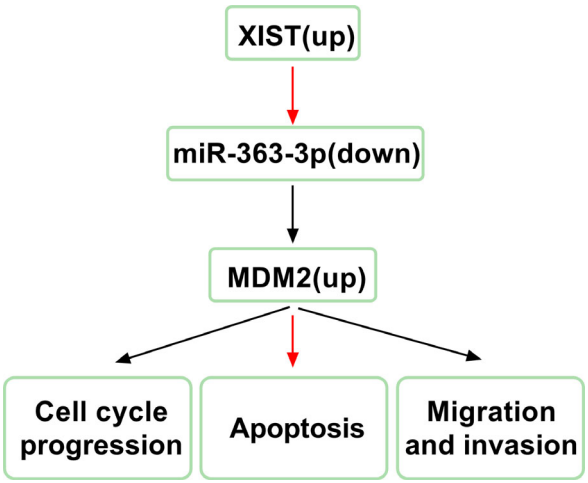

Figure 7 A schematic diagram of XIST in the progression of LAD. Upregulation of XIST facilitated migration, invasion and cell cycle progression, and curbed apoptosis of LAD cells through enhancing MDM2 expression via downregulating miR-363-3p. (⟶) Inhibit, (⟶) Promote.

Acknowledgment

This work was supported by National Natural Science Foundation of China (Grant No.81802325).

Disclosure

The authors have no conflict of interest to declare.

References

1 Bray F, Ferlay J, Soerjomataram I, Siegel RL, Torre LA, Jemal A. Global cancer statistics 2018: GLOBOCAN estimates of incidence and mortality worldwide for 36 cancers in 185 countries. *CA Cancer J Clin* 2018; **68**: 394–424.
2 Ferlay J, Shin HR, Bray F, Forman D, Mathers C, Parkin DM. Estimates of worldwide burden of cancer in 2008: GLOBOCAN 2008. *Int J Cancer* 2010; **127**: 2893–917.
3 Tian X, Zhang H, Zhang B, Zhao J, Li T, Zhao Y. Microarray expression profile of long non-coding RNAs in paclitaxel-resistant human lung adenocarcinoma cells. *Oncol Rep* 2017; **38**: 293–300.
4 Siegel RL, Miller KD, Jemal A. Cancer statistics, 2016. *CA Cancer J Clin* 2016; **66**: 7–30.
5 Zhang H, Chen Z, Wang X, Huang Z, He Z, Chen Y. Long non-coding RNA: A new player in cancer. *J Hematol Oncol* 2013; **6**: 37.
6 Lu Z, Carter AC, Chang HY. Mechanistic insights in X-chromosome inactivation. *Philos Trans R Soc Lond B Biol Sci* 2017; **372**: 20160356.
7 Chen DL, Chen LZ, Lu YX *et al.* Long noncoding RNA XIST expedites metastasis and modulates epithelial-mesenchymal transition in colorectal cancer. *Cell Death Dis* 2017; **8**: e3011.
8 Chen DL, Ju HQ, Lu YX *et al.* Long non-coding RNA XIST regulates gastric cancer progression by acting as a molecular sponge of miR-101 to modulate EZH2 expression. *J Cell Biochem* 2016; **35**: 142.
9 Wei W, Liu Y, Lu Y, Yang B, Tang L. LncRNA XIST promotes pancreatic cancer proliferation through miR-133a/EGFR. *J Cell Biochem* 2017; **118**: 3349–58.
10 Kong Q, Zhang S, Liang C *et al.* LncRNA XIST functions as a molecular sponge of miR-194-5p to regulate MAPK1 expression in hepatocellular carcinoma cell. *J Cell Biochem* 2018; **119**: 4458–68.
11 Sun J, Pan LM, Chen LB, Wang Y. LncRNA XIST promotes human lung adenocarcinoma cells to cisplatin resistance via let-7i/BAG-1 axis. *Cell Cycle* 2017; **16**: 2100–7.
12 Cai Y, Yu X, Hu S, Yu J. A brief review on the mechanisms of miRNA regulation. *Genomics Proteomics Bioinformatics* 2009; **7**: 147–54.
13 Fabien MR, Sonenberg N, Filipowicz W. Regulation of mRNA translation and stability by microRNAs. *Annu Rev Biochem* 2010; **79**: 351–79.
14 Boguslawska J, Rodzik K, Poplawski P *et al.* TGF-beta1 targets a microRNA network that regulates cellular adhesion and migration in renal cancer. *Cancer Lett* 2018; **412**: 155–69.
15 Liu J, Li Q, Li R, Ren P, Dong S. MicroRNA-363-3p inhibits papillary thyroid carcinoma progression by targeting PIK3CA. *Am J Cancer Res* 2017; **7**: 148–58.
16 Wang K, Yan L, Lu F. miR-363-3p inhibits osteosarcoma cell proliferation and invasion via targeting SOX4. *Oncol Res* 2019; **27**: 157–63.
17 Hu F, Min J, Cao X *et al.* MiR-363-3p inhibits the epithelial-to-mesenchymal transition and suppresses metastasis in colorectal cancer by targeting Sox4. *Biochem Biophys Res Commun* 2016; **474**: 35–42.
18 Bian WG, Zhou XN, Song S, Chen HT, Shen Y, Chen P. Reduced miR-363-3p expression in non-small cell lung cancer is associated with gemcitabine resistance via targeting of CUL4A. *Eur Rev Med Pharmacol Sci* 2019; **23**: 649–59.
19 Chang J, Gao F, Chu H, Lou L, Wang H, Chen Y. miR-363-3p inhibits migration, invasion, and epithelial-mesenchymal transition by targeting NEDD9 and SOX4 in non-small-cell lung cancer. *J Cell Physiol* 2019; **235**: 1808–1820.
20 Honda R, Tanaka H, Yasuda H. Oncoprotein MDM2 is a ubiquitin ligase E3 for tumor suppressor p53. *FEBS Lett* 1997; **420**: 25–7.
21 Momand J, Zambetti GP, Olson DC, George D, Levine AJ. The mdm-2 oncogene product forms a complex with the p53 protein and inhibits p53-mediated transactivation. *Cell* 1992; **69**: 1237–45.
22 Meng X, Franklin DA, Dong J, Zhang Y. MDM2-p53 pathway in hepatocellular carcinoma. *Cancer Res* 2014; **74**: 7161–7.

23 Qiu W, Xia X, Qiu Z, Guo M, Yang Z. RasGRP3 controls cell proliferation and migration in papillary thyroid cancer by regulating the Akt-MDM2 pathway. *Gene* 2017; **633**: 35–41.
24 Chen Y, Wang DD, Wu YP *et al*. MDM2 promotes epithelial-mesenchymal transition and metastasis of ovarian cancer SKOV3 cells. *Br J Cancer* 2017; **117**: 1192–201.
25 Tang Y, Xuan Y, Qiao G *et al*. MDM2 promotes epithelial-mesenchymal transition through activation of Smad2/3 signaling pathway in lung adenocarcinoma. *Onco Targets Ther* 2019; **12**: 2247–58.
26 Denisenko TV, Budkevich IN, Zhivotovsky B. Cell death-based treatment of lung adenocarcinoma. *Cell Death Dis* 2018; **9**: 117.
27 Huarte M. The emerging role of lncRNAs in cancer. *Nat Med* 2015; **21**: 1253–61.
28 Chandra Gupta S, Nandan TY. Potential of long non-coding RNAs in cancer patients: From biomarkers to therapeutic targets. *Int J Cancer* 2017; **140**: 1955–67.
29 Tay Y, Rinn J, Pandolfi PP. The multilayered complexity of ceRNA crosstalk and competition. *Nature* 2014; **505**: 344–52.
30 Jiang C, Cao Y, Lei T *et al*. microRNA-363-3p inhibits cell growth and invasion of nonsmall cell lung cancer by targeting HMGA2. *Mol Med Rep* 2018; **17**: 2712–8.
31 Bartel DP. MicroRNAs: Target recognition and regulatory functions. *Cell* 2009; **136**: 215–33.
32 Zhang DH, Zhang LY, Liu DJ, Yang F, Zhao JZ. Expression and significance of MMP-9 and MDM2 in the oncogenesis of lung cancer in rats. *Asian Pac J Trop Med* 2014; **7**: 585–8.

